Eur J Nucl Med Mol Imaging (2009) 36:73–80
DOI 10.1007/s00259-008-0919-6

ORIGINAL ARTICLE

Uptake of inflammatory cell marker [^{11}C]PK11195 into mouse atherosclerotic plaques

Iina Laitinen · Päivi Marjamäki · Kjell Någren · V. Jukka O. Laine · Ian Wilson · Pia Leppänen · Seppo Ylä-Herttuala · Anne Roivainen · Juhani Knuuti

Received: 30 April 2008 / Accepted: 1 August 2008 / Published online: 19 August 2008

Abstract
Purpose The ligand [^{11}C]PK11195 binds with high affinity and selectivity to peripheral benzodiazepine receptor, expressed in high amounts in macrophages. In humans, [^{11}C]PK11195 has been used successfully for the in vivo imaging of inflammatory processes of brain tissue. The purpose of this study was to explore the feasibility of [^{11}C]PK11195 in imaging inflammation in the atherosclerotic plaques.
Methods The presence of PK11195 binding sites in the atherosclerotic plaques was verified by examining the in vitro binding of [^{3}H]PK11195 onto mouse aortic sections. Uptake of intravenously administered [^{11}C]PK11195 was studied ex vivo in excised tissue samples and aortic sections of a LDLR/ApoB48 atherosclerotic mice. Accumulation of the tracer was compared between the atherosclerotic plaques and non-atherosclerotic arterial sites by autoradiography and histological analyses.
Results The [^{3}H]PK11195 was found to bind to both the atherosclerotic plaques and the healthy wall. The autoradiography analysis revealed that the uptake of [^{11}C]PK11195 to inflamed regions in plaques was more prominent (p= 0.011) than to non-inflamed plaque regions, but overall it was not higher than the uptake to the healthy vessel wall. Also, the accumulation of ^{11}C radioactivity into the aorta of the atherosclerotic mice was not increased compared to the healthy control mice.
Conclusions Our results indicate that the uptake of [^{11}C]PK11195 is higher in inflamed atherosclerotic plaques containing a large number of inflammatory cells than in the non-inflamed plaques. However, the tracer uptake to other structures of the artery wall was also prominent and may limit the use of [^{11}C]PK11195 in clinical imaging of atherosclerotic plaques.

Keywords Atherosclerosis · Autoradiography · Biodistribution · Cardiology molecular imaging · ^{11}C-PK11195

I. Laitinen (✉) · P. Marjamäki · K. Någren · A. Roivainen · J. Knuuti
Turku PET Centre, University of Turku,
Kiinamyllynkatu 4–8,
FI-20520 Turku, Finland
e-mail: iina.laitinen@tyks.fi

V. J. O. Laine
Department of Pathology, Turku University Hospital,
Turku, Finland

I. Wilson
Medical Diagnostics, GE Healthcare Biosciences,
London, UK

P. Leppänen · S. Ylä-Herttuala
A.I. Virtanen Institute, University of Kuopio,
Kuopio, Finland

Introduction

Atherosclerotic plaque rupturing is considered an important determinant of the outcome of coronary artery disease. Identifying vulnerable plaques that are prone to rupture is, therefore, of great clinical interest. High concentrations of inflammatory cells, mainly macrophages, has been suggested to be one characteristic of the vulnerable plaques [1–3].

The metabolic activity and inflammatory processes of atherosclerotic plaques in humans and animal models have recently been detected using fluorine-18-labelled fluorodeoxyglucose ([^{18}F]FDG) in positron emission tomography

(PET) [4–7]. Despite these promising results, other imaging markers are warranted since [^{18}F]FDG has obvious limitations for cardiac imaging, such as high accumulation to myocardium and dependence on metabolic conditions of the patient.

[^{11}C]PK11195 binds with high affinity and selectivity to peripheral benzodiazepine receptor (PBR, also known as translocator protein) [8, 9]. The PBR is widely expressed in the body and, although it has been found in all cell types studied, the expression levels in different cell types vary. PBR is expressed in high amounts in macrophages, the number of PK binding sites in macrophages is estimated to 250,000 per cell [10, 11]. Little information is known about the numbers of PBR in other cell types, but its relative expression is highest in glandular tissues, lung and myocardium [12, 13] and to a lesser extent in other tissues including the endothelial and smooth muscle cells in the blood vessels [14]. Ligands for PBR have been used successfully for the imaging of degenerative brain diseases, based on the low expression of PBR in the normal brain tissue and high expression of PBR in activated glial cells and infiltrated macrophages. Also, in the periphery, PBR are highly expressed in activated macrophages in the inflamed area.

[^{11}C]PK11195 has previously been found to accumulate into the inflamed lung in animal models [15, 16] and in humans [17] due to the high number of activated macrophages in the inflamed area. A microautography study by Jones et al. [16] shows selective high binding of ^{3}H-labelled PK to macrophages in an inflammatory cell mixture, already at a time point of 10 min. According to these studies, the macrophage express the highest number of PK binding sites among the inflammatory cells. Therefore, [^{11}C]PK11195 has promising qualities as an imaging agent also in atherosclerosis-associated inflammation.

In this study, the feasibility of labelled PK11195 in the assessment of the inflammation in the arterial atherosclerotic plaques was studied both in vitro and ex vivo by using [^{3}H]PK11195 and [^{11}C]PK11195 and aortic sections of a LDLR/ApoB48 atherosclerotic mice. By combining autoradiography with histological and the immunohistological analyses, the accumulation of the tracer was compared between the atherosclerotic plaques and non-atherosclerotic arterial sites.

Materials and methods

Animals

Five male mice deficient for both LDL receptor and ApoB48 (LDLR$^{-/-}$/ApoB$^{100/100}$, Jackson Laboratory strain #003000) were investigated. LDLR/ApoB48-deficient mice were chosen as a model because these animals show a high prevalence of atherosclerotic plaques [4, 18–20]. Starting at 10 months of age, the mice were kept on a Western-type diet (Teklad Adjusted Calories, consisting of 21% fat and 0.15% cholesterol without sodium cholate) for 3 months. The C57Bl/6N strain male mice (n=3) fed with a standard diet were used as non-atherosclerotic controls. The age and weight (mean±SD) of the LDLR/ApoB48 mice were 13±1 months and 39±8 g, respectively, and of the C57BL/6N control mice were 9 months and 28±4 g, respectively. All mice were maintained under standard conditions. Food and water were provided ad libitum. The study plan was approved by the Laboratory Animal Care and Use Committee of the University of Turku, Finland.

Radiotracer synthesis

[^{11}C]PK11195 was prepared as described by Debruyne et al. [21] with slight modifications. [^{11}C]Methyl iodide was let to react with 1.0 mg of desmethyl-PK11195 (ABX, Radeberg, Germany) and 3.0 μL of 1.0 M tetrabutylammonium hydroxide in 150 μL of dimethyl sulfoxide for 3 min at 80°C. The crude product was purified on a semi-preparative μ-Bondapak® C-18 column using 65% of acetonitrile in 10 mM phosphoric acid. After evaporation of the high-performance liquid chromatography (HPLC) solvent, the purified product was formulated in propylene glycol/ethanol, 7/3, and 0.1 M phosphate buffer, pH 7.4, and filtered through a 0.22-μm sterile filter. Measurement of concentration and radiochemical purity of [^{11}C]PK11195 batches was performed by HPLC using an analytical μ-Bondapak® C-18 column, a UV-detector set at 223 nm and a radioactivity detector in series. Radiochemical purity was higher than 99.5%.

In vitro binding of [^{3}H]PK11195 in aorta sections

Twenty-micrometer sections of atherosclerotic mouse aorta were prepared [4] and stored at −20°C. Before use, the sections were warmed to room temperature (RT) and pre-incubated for 5 min at RT in 50 mM Tris–HCl buffer (pH 7.4). Immediately thereafter, the sections were incubated for 30 min at RT with 1.2 nM [^{3}H]PK11195 (85 Ci/mmol; Amersham, SA) in 50 mM Tris–HCl buffer. Non-specific binding was estimated in adjacent sections in the presence of 10 μM (unlabelled) PK11195 (ABX, Radeberg, Germany). After incubation, the slides were washed twice for 10 s with ice-cold buffer and rinsed in distilled water to remove buffer salts. The sections were air-dried and apposed to an imaging plate (Fuji Imaging Plate BAS-TR2025, Fuji Photo Film, Japan) for digital autoradiography. The exposure time was 7 days. The imaging plates were scanned with the Fuji Analyzer BAS-5000. The digital autoradiographic images were analysed for count

densities (photo-stimulated luminescence unit per area, PSL/mm^2) with a computerised image analysis programme (Tina 2.1, Raytest Isotopenmessgeräte, Straubenhardt, Germany) and the count densities for background areas were subtracted from the image data.

Ex vivo biodistribution of [^{11}C]PK11195 in atherosclerotic and control mice

[^{11}C]PK11195 (23±12 MBq) was given intravenously via a tail vein to non-anaesthetised mice, and after 20 min, the animals were killed by CO_2. Blood was immediately collected by cardiac puncture into heparinised tubes, weighed and measured for [^{11}C]radioactivity in a calibrated well counter (NaI(Tl) 3×3 in., Bicron 3 MW3/3P, Bicron, Newbury, OH, USA). Tissue samples (aorta, lung, liver and heart) were dissected, patted dry, weighed and their radioactivity were measured. Background counts were subtracted and the radioactivity decay was corrected to the time of injection, and the dose that remained in the tail was compensated. The radioactivity that had accumulated in the tissue samples over the 20-min period following [^{11}C] PK11195 injection was expressed as a percentage of the injected dose per gram of tissue (%ID/g).

Uptake of [^{11}C]PK11195 in aorta sections ex vivo

The distribution of [^{11}C]PK11195 to aorta tissue was studied with digital autoradiography. The aorta from the ascending aorta to the level of the diaphragm was dissected and blood was removed with saline rinsing. The aortas were frozen in mounting media for sectioning with cryomicrotome. Sequential longitudinal 20 μm mouse aorta sections were cut at −15°C, thaw-mounted onto microscope slides, air-dried and apposed to an imaging plate (Fuji Imaging Plate BAS-TR2025, Fuji Photo Film, Japan). After an exposure time of 1 h, the imaging plates were scanned with the Fuji Analyzer BAS-5000 and the images were analysed for count densities (PSL/mm^2) with an image analysis programme (Tina 2.1, Raytest Isotopenmessgeräte, Straubenhardt, Germany). Three types of regions of interest (ROI) were defined according to the histology [22], and the background area count densities were subtracted from the image data. The ROIs were (1) healthy vessel wall (control site, no visual progression of atherosclerosis), (2) non-inflamed plaque (mostly core areas without cell infiltration or acellular areas in the plaque) and (3) inflamed plaque (cell-rich areas in the plaques containing mostly macrophages). The ROI were drawn with the help of a microscope on carefully co-registered images. Analysis was also performed on adjacent sections adding the effect of repeated measurement. The mean values for intensities (PSL/mm^2 values) were calculated.

Histology

After autoradiography, the sections were stained in haematoxylin and eosin and studied for morphology. The degree of inflammation in the whole aortic tissue was semi-quantitatively assessed by an experienced pathologist as the number of leucocytes in the tissue (no leucocytes = non-inflamed aorta; occasional single polymorphonuclear leucocytes or lymphocytes = mild inflammation; occasional polymorphonuclear leucocytes or lymphocytes and some groups of inflammatory cells = moderate inflammation; abundant infiltration of polymorphonuclear leucocytes and/or lymphocytes = severe inflammation) [4]. For ROI analysis, each plaque area was defined according to the histology as non-inflamed (none or occasional leucocytes) or inflamed (moderate or severe inflammation).

Adjacent sections were immunostained with Mac-3 (antibody for mouse macrophages) and PBR antibody. Eight micrometer sections stored at −70°C were melted, air-dried and fixed in ice-cold acetone. Endogenous peroxidase was blocked and the sections were incubated for 1 h with Mac-3 antibody. Control immunostaining was performed with IgG-negative control antibody. Biotinylated secondary antibody was incubated for 30 min, followed by incubations with streptavidin–horseradish peroxidase and AEC Substrate Chromogen according to the instructions of the manufacturer. Finally, the sections were counterstained in haematoxylin. All antibodies were from BD Pharmingen and all reagents were from DakoCytomation, CA, USA.

Statistical methods

All results are expressed as the mean±SD. Univariate correlations were calculated using the Spearman correlation method. Analysis of variance (ANOVA) was used to study the significance of differences observed in animal characteristics and biodistribution between LDLR/ApoB48 mice and control animal groups. In autoradiography analysis, parametric ANOVA of repeated measures was used in the inter-animal comparison for the mean PSL values of radioactive uptake of defined ROI. For intra-animal comparisons, ANOVA was used. A p value less than 0.05 was considered as statistically significant.

Results

Characterisation of atherosclerosis in LDLR/ApoB48 mice

All LDLR/ApoB48 mice had extensive atherosclerosis showing plaques with different characteristics throughout the aortic tree. The observed plaques in the aorta contained cell-rich, inflamed areas and acellular necrotic cores, mostly

resembling type V lesions [22]. Leucocyte infiltration was observed in plaques in all mice and, based on the histological analysis, the inflammation was estimated to be of a moderate degree (occasional polymorphonuclear leucocytes or lymphocytes and some groups of inflammatory cells). Macrophage staining revealed areas in the plaques with moderate number of macrophages and PBR-specific antibody stained mainly the same sites as the macrophage antibody (Fig. 1). In control mice aortas, no atherosclerosis was detected.

Binding of [^{3}H]PK11195 in aortic sections

The presence of PK11195 binding sites in the atherosclerotic plaques was verified by examining the in vitro competive binding of tritium-labelled PK11195 onto aortic sections (41 sections from five mice). [^{3}H]PK11195 was found to bind to the aortic sections in the sites of the plaques and also on the healthy wall (Fig. 2). The specific vs. non-specific binding ratio was high (12-fold).

Aortic uptake and biodistribution of [^{11}C]PK11195 in LDLR/ApoB48 and control mice

The uptake of [^{11}C]PK11195 in the whole aorta of atherosclerotic LDLR/ApoB48 mice (4.96±0.16%ID/g, n=5) was significantly lower than that in the control mice (9.00±0.12%ID/g, n=3) (p=0.004) (Table 1). In plasma, lung and heart, the [^{11}C]PK11195 uptake did not differ between the controls and the LDLR/ApoB48 mice. The availability of [^{11}C]PK11195 in the circulating blood was not found to be affected by the animal weight (p=0.26). The uptake ratio of aorta to plasma was 22±7 and aorta to heart was 0.6±0.3 in LDLR/ApoB48 mice.

Distribution of [^{11}C]PK11195 in aortic sections

In the longitudinal sections of the aorta, both healthy vessel wall and atherosclerotic plaques were found. Autoradiograms of nine to 12 sections of each animal were analysed. In total, 136 non-inflamed plaque regions, 279 inflamed plaque regions and 147 healthy vessel wall regions were analysed from autoradiograms (Figs. 3 and 4). In each mouse, the mean uptake of [^{11}C]-radioactivity into each region were calculated (Table 2).

Autoradiography analysis revealed diffuse [^{11}C]PK11195 uptake in the aorta sections, which was not specifically limited to the inflamed plaques. There was significantly higher accumulation of ^{11}C radioactivity to the inflamed regions compared to the non-inflamed regions of the plaques (p=0.011), but no difference in the accumulation in the inflamed regions and the healthy vessel wall of the same animals was found. The uptake to cell-rich sites in plaques did not differ from the uptake to the healthy vessel wall (p=0.1) (Table 2).

Discussion

The aim of this study was to investigate the uptake of [^{11}C]PK11195 in atherosclerotic plaques of the LDLR/ApoB48 mice and estimate its potential to be used in the imaging of inflammation associated with atherosclerosis. We found that the uptake of tracer was higher in the inflamed atherosclerotic plaques than in the non-inflamed plaques. However, the tracer uptake to other structures of the artery wall, to both healthy wall and adventitial tissue was also evident and comparable to the uptake into the inflamed plaques. This suggests that clinical imaging of vascular inflammatory processes with [^{11}C]PK11195 is challenging and a tracer with a better target-to-background ratio would be likely needed.

The presence of PK11195 binding sites in the atherosclerotic plaques was verified in an in vitro setting. In the displacement studies, the binding of [^{3}H]PK11195 was found to be specific. However, already in these studies, [^{3}H]PK11195 was found to bind to the healthy artery wall in addition to plaques. In the subsequent ex vivo studies, also quite diffuse [^{11}C]PK11195 uptake was seen, not specifically limited to the inflamed plaques. This finding

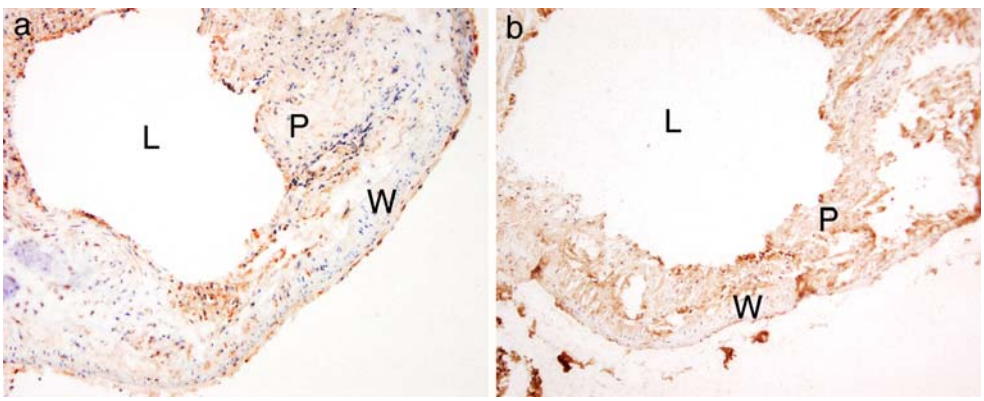

Fig. 1 A plaque in the brachiocephalic artery trunk, concecutive sections. **a** Macrophage staining (Mac-3) and **b** PBR-specific antibody. *L* lumen, *P* plaque, *W* wall. Original magnification ×100

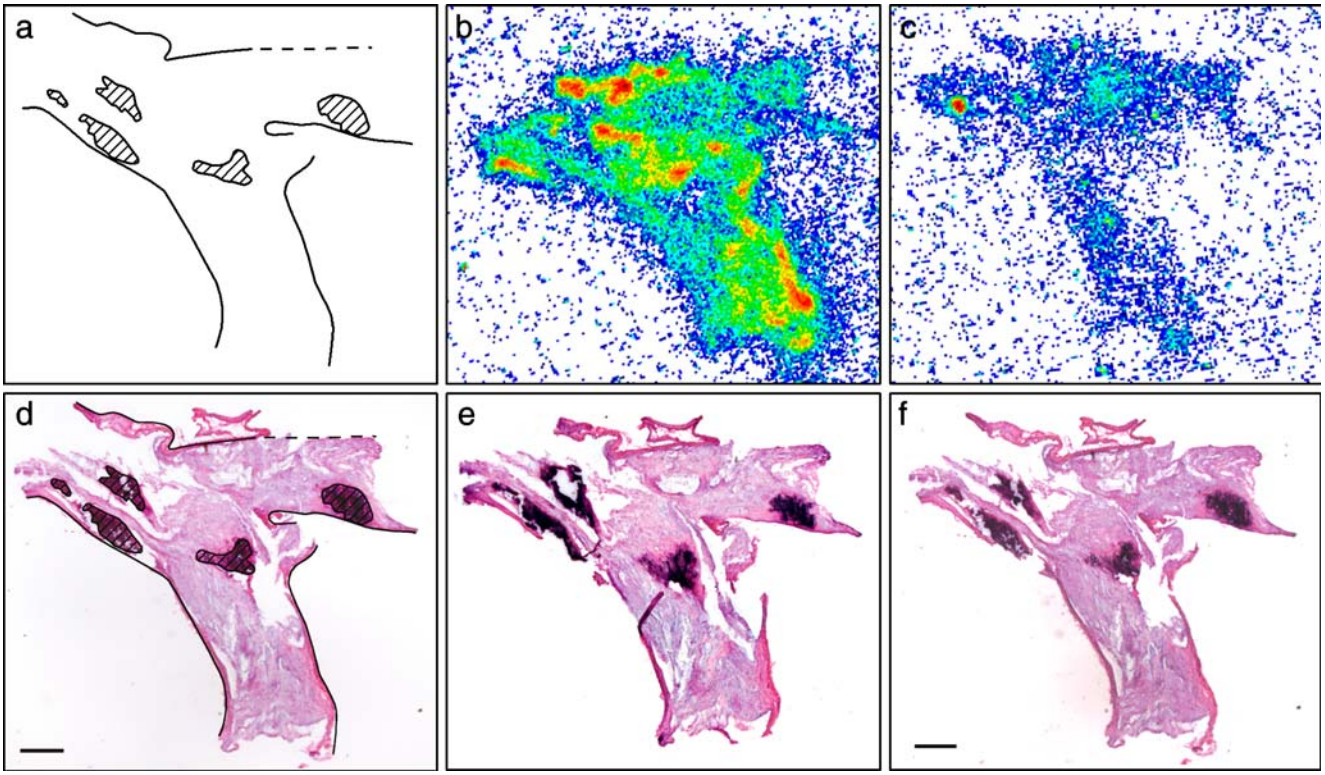

Fig. 2 **a** Contour image of a section of atherosclerotic mouse aorta; **b** in vitro binding of [^{3}H]PK11195; **c** adjacent section, in vitro [^{3}H] PK11195 with a blocking dose of cold PK11195; **d–f** representative sections, HE stain. Bar=0.4 mm

was supported by the results that the uptake of [^{11}C] PK11195 (%ID/g) was not higher in the aorta of atherosclerotic mice compared to the control mice.

PK11195 is a high-affinity ligand to PBR. PBR, also known as translocator protein [8], is present in the mitochondrial outer membrane as a part of the complex formed by voltage-dependent anion channel and adenine nucleotide transporter [23]. Relatively high expression of PBR can be found in leucocytes especially in monocyte/macrophages and neutrophils but it is also expressed in adrenal gland, lung, kidney and heart, and in other tissues in lesser amounts [10, 11, 24]. In the brain, PBR can only be found in low numbers in the glial cells and astrocytes, but in neurodegenerative states, the activated glial cells express high amounts of PBR [25]. [^{11}C]PK11195 has previously been used for PET imaging of inflammation related to multiple sclerosis [21], and it has also been suggested as a suitable agent for the imaging of atherosclerosis-associated inflammation. The accumulation in the inflamed lung in animal models and humans [15–17] have been shown to be

Table 1 The biodistribution [%ID/g (mean±SD)] of intravenously administered [^{11}C]PK11195 in atherosclerotic LDLR/ApoB48 mice and control C57Bl/6N mice

	LDLR/ApoB48 (n=5)	C57Bl/6N (n=3)	p value[a]
Aorta	4.96±1.29	9.00±1.11	0.004
Heart	9.24±2.38	11.95±0.31	NS
Liver	5.27±2.35	9.28±0.76	0.032
Lung	29.71±9.64	28.74±1.29	NS
Plasma	0.22±0.03	0.26±0.03	NS

[a] Difference between atherosclerotic and control mice

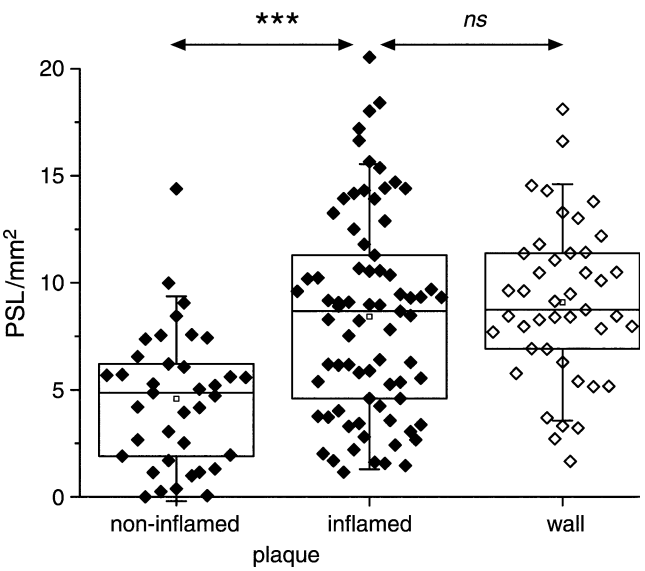

Fig. 3 Example of autoradiography analysis (mouse no. 108)

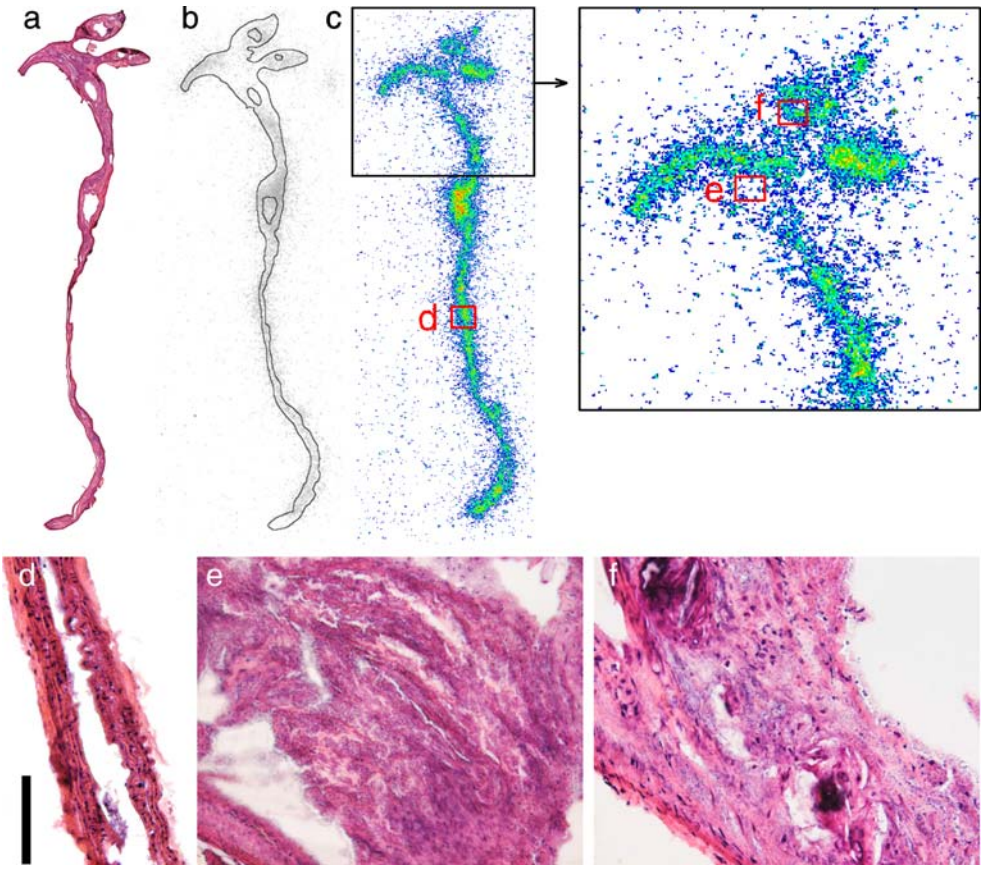

Fig. 4 An example of analysis of the aortic sections. **a** HE stain of the section, **b** autoradiography image with superimposed contour image, **c** ARG image, **d** healthy vessel wall, **e** non-inflamed plaque region, **f** inflamed plaque region. Original magnification ×200 (**d**–**f**), scale bar=100 μm

significantly increased due to activated macrophages in the inflamed area.

It is possible that macrophages may express PBR differently in response to their environment. A very recent report by Branley et al. shows that, although [^{3}H]PK11195 binds solely to macrophages of bronchoalveolar lavage cells in patients with interstitial lung disease (ILS), the total binding in the lung is diminished compared to healthy controls [26]. They suggest that, in ILS and in other inflammatory diseases like osteoarthritis [27], the reduced expression of PBR in the macrophages may be a reflection of a proapoptotic and proinflammatory milieu. We do not know the amount of PBR specifically in the macrophages in the atherosclerotic plaques, but it is possible that although the macrophages are present in the plaques, the level of PBR expression may differ as a reflection of their altered functionality and environment.

Table 2 Autoradiography analysis of accumulated radioactivity into vascular areas in LDLR/ApoB48 mice. The intensity (PSL/mm^2, mean±SD)

No.	Plaque		Healthy wall
	Non-inflamed	Inflamed	
106	11.4±11.9 (n=23)	14.1±10.2 (n=55)	19.8±7.0 (n=21)
108	4.6±3.2 (n=37)	8.3±4.6 (n=75)	9.1±3.7 (n=43)
109	2.6±1.9 (n=28)	5.6±2.8 (n=57)	5.8±2.2 (n=19)
112	1.8±1.0 (n=25)	3.7±2.2 (n=54)	4.7±2.3 (n=30)
114	40.7±16.9 (n=23)	40.3±28.0 (n=38)	62.8±23.0 (n=34)

Inter-animal comparison showed significant difference (p=0.011) between non-inflamed and inflamed regions in plaques, but no significant difference between inflamed plaques and healthy wall

In this study, the uptake of [^{11}C]PK11195 in the whole aorta of atherosclerotic LDLR/ApoB48 mice was found to be lower compared to the aortas of the C57Bl control mice. This could be explained by the high number and mass of core areas of the plaques observed in the aorta of atherosclerotic mice. As autoradiography analysis showed, [^{11}C]PK11195 does not accumulate to these non-inflamed sites. The atherosclerotic aortas have higher mass due to these plaques, and therefore, the radioactivity calculated against the weight per gram tissue is lower when accumulation in other sites is similar.

Limitations

The biodistribution studies were performed at one time point of 20 min. [^{11}C]PK11195 has been found to metabolise rapidly in vivo in mice and humans [28]. According to our studies, 20 min after injection, the amount of unchanged [^{11}C]PK11195 was 78% in human plasma and 85% in rat plasma [29]. In this study, we chose to use a time point of

20 min due to the short half-life of ^{11}C and detection difficulties of samples of small size. With a longer time point, the target-to-background ratio might have been better, although at the time point of 20 min, the tissue-to-blood ratios were already very good.

The physiological differences between the controls and atherosclerotic mice may explain the observed variance in the uptake of [^{11}C]PK11195 in the aorta. In the biodistribution study, the animal weight was not considered to be a source of bias since the availability of [^{11}C]PK11195 in the circulating blood was not affected by the animal weight (p=0.26). However, there was a significant difference in the uptake of [^{11}C]PK11195 in the liver. LDLR/ApoB48 mice could suffer from compromised liver functions due to atherosclerosis and high plasma lipid levels, which could affect the uptake in the liver. As for the other studied tissues (plasma, erythrocytes, lung and heart), the [^{11}C]PK11195 uptake did not differ between the controls and the LDLR/ApoB48 mice.

The variance in the ROI analysis may partly be due to the small size of the analysed areas, especially in the healthy vessel wall, which is only a few cell layers in thickness. Interference from other nearby tissue compartments was, however, diminished by drawing ROIs for the healthy wall region farther away from the plaques. The variance observed in the plaque ROIs may be partly due to the heterogenity of cellular composition in the 20-μm sections. Macrophages were detected in the plaques by comparing the HE-stained autoradiography sections to consecutive macrophage-stained sections and directly from HE-stained sections by morphology. The inflammatory activity was defined based on the information of the consecutive macrophage-stained section and cellularity of the site in these advanced plaques and the macrophages were not specifically counted, therefore, these sites may contain also other leucocytes and occasional smooth muscle cells. However, for clinical application, it is more important to differentiate the active, cell-rich, inflamed plaques from non-inflamed plaques, since these are pathologically very different and their vulnerability prognosis is essentially different.

Conclusions

Our results indicate that the uptake of [^{11}C]PK11195 to the atherosclerotic vessels is not limited to inflamed plaques. In a mouse model of atherosclerosis, the uptake to inflamed regions in plaques was more prominent than to non-inflamed areas, but did not differ from the uptake to the healthy vessel wall. This binding to surrounding tissue resulting in high background may limit the usability of [^{11}C]PK11195 in clinical imaging of atherosclerotic plaques.

Aknowledgements This work was funded by Ida Montin Foundation, Finnish Cultural Foundation, Turku University Foundation, Aarne Koskelo Foundation, Finnish Foundation for Cardiovascular Research and the Hospital District of Southwest Finland. The study is also partly supported by the Finnish Centre of Excellence in Molecular Imaging in Cardiovascular and Metabolic Research. The authors would like to thank adjunct professor Merja Haaparanta-Solin for revising the manuscript, Tarja Marttila and Marko Vehmanen for the technical assistance and M.Sc. Irina Lisinen for the statistical analysis.

Conflict of interest statement The authors declare that they have no conflict of interest.

References

1. Jander S, Sitzer M, Schumann R, Schroeter M, Siebler M, Steinmetz H, et al. Inflammation in high-grade carotid stenosis: a possible role for macrophages and T cells in plaque destabilization. Stroke 1998;29:1625–30.
2. Moreno PR, Bernardi VH, Lopez-Cuellar J, Murcia AM, Palacios IF, Gold HK, et al. Macrophages, smooth muscle cells, and tissue factor in unstable angina. Implications for cell-mediated thrombogenicity in acute coronary syndromes. Circulation 1996;94:3090–7.
3. Naghavi M, Libby P, Falk E, Casscells SW, Litovsky S, Rumberger J, et al. From vulnerable plaque to vulnerable patient: a call for new definitions and risk assessment strategies: part I. Circulation 2003; 108:1664–72.
4. Laitinen I, Marjamäki P, Haaparanta M, Savisto N, Laine VJ, Soini SL, et al. Non-specific binding of [18F]FDG to calcifications in atherosclerotic plaques: experimental study of mouse and human arteries. Eur J Nucl Med Mol Imaging 2006;33:1461–7.
5. Ogawa M, Ishino S, Mukai T, Asano D, Teramoto N, Watabe H, et al. [18F]-FDG accumulation in atherosclerotic plaques: immunohistochemical and PET imaging study. J Nucl Med 2004;45: 1245–50.
6. Rudd JH, Warburton EA, Fryer TD, Jones HA, Clark JC, Antoun N, et al. Imaging atherosclerotic plaque inflammation with [18F]-fluorodeoxyglucose positron emission tomography. Circulation 2002; 105:2708–11.
7. Tawakol A, Migrino RQ, Hoffmann U, Abbara S, Houser S, Gewirtz H, et al. Noninvasive in vivo measurement of vascular inflammation with F-18 fluorodeoxyglucose positron emission tomography. J Nucl Cardiol 2005;12:294–301.
8. Papadopoulos V, Baraldi M, Guilarte TR, Knudsen TB, Lacapere JJ, Lindemann P, et al. Translocator protein (18kDa): new nomenclature for the peripheral-type benzodiazepine receptor based on its structure and molecular function. Trends Pharmacol Sci 2006;27:402–9.
9. Le Fur G, Guilloux F, Rufat P, Benavides J, Uzan A, Renault C, et al. Peripheral benzodiazepine binding sites: effect of PK 11195, 1-(2-chlorophenyl)-*N*-methyl-(1-methylpropyl)-3 isoquinolinecarboxamide. II. In vivo studies. Life Sci 1983;32:1849–56.
10. Canat X, Carayon P, Bouaboula M, Cahard D, Shire D, Roque C, et al. Distribution profile and properties of peripheral-type benzodiazepine receptors on human hemopoietic cells. Life Sci 1993;52:107–18.
11. Zavala F, Haumont J, Lenfant M. Interaction of benzodiazepines with mouse macrophages. Eur J Pharmacol 1984;106:561–6.
12. Anholt RR, De Souza EB, Oster-Granite ML, Snyder SH. Peripheral-type benzodiazepine receptors: autoradiographic localization in whole-body sections of neonatal rats. J Pharmacol Exp Ther 1985;233:517–26.
13. Parola AL, Yamamura HI, Laird HE III. Peripheral-type benzodiazepine receptors. Life Sci 1993;52:1329–42.

14. Veenman L, Gavish M. The peripheral-type benzodiazepine receptor and the cardiovascular system. Implications for drug development. Pharmacol Ther 2006;110:503–24.
15. Hardwick MJ, Chen MK, Baidoo K, Pomper MG, Guilarte TR. In vivo imaging of peripheral benzodiazepine receptors in mouse lungs: a biomarker of inflammation. Mol Imaging 2005;4:432–8.
16. Jones HA, Valind SO, Clark IC, Bolden GE, Krausz T, Schofield JB, et al. Kinetics of lung macrophages monitored in vivo following particulate challenge in rabbits. Toxicol Appl Pharmacol 2002;183:46–54.
17. Jones HA, Marino PS, Shakur BH, Morrell NW. In vivo assessment of lung inflammatory cell activity in patients with COPD and asthma. Eur Respir J 2003;21:567–73.
18. Heinonen SE, Leppänen P, Kholova I, Lumivuori H, Häkkinen SK, Bosch F, et al. Increased atherosclerotic lesion calcification in a novel mouse model combining insulin resistance, hyperglycemia, and hypercholesterolemia. Circ Res 2007;101:1058–67.
19. Leppänen P, Koota S, Kholova I, Koponen J, Fieber C, Eriksson U, et al. Gene transfers of vascular endothelial growth factor-A, vascular endothelial growth factor-B, vascular endothelial growth factor-C, and vascular endothelial growth factor-D have no effects on atherosclerosis in hypercholesterolemic low-density lipoprotein-receptor/apolipoprotein B48-deficient mice. Circulation 2005;112:1347–52.
20. Veniant MM, Pierotti V, Newland D, Cham CM, Sanan DA, Walzem RL, et al. Susceptibility to atherosclerosis in mice expressing exclusively apolipoprotein B48 or apolipoprotein B100. J Clin Invest 1997;100:180–8.
21. Debruyne JC, Versijpt J, Van Laere KJ, De Vos F, Keppens J, Strijckmans K, et al. PET visualization of microglia in multiple sclerosis patients using [11C]PK11195. Eur J Neurol 2003;10:257–64.
22. Stary HC, Chandler AB, Dinsmore RE, Fuster V, Glagov S, Insull W Jr., et al. A definition of advanced types of atherosclerotic lesions and a histological classification of atherosclerosis. A report from the Committee on Vascular Lesions of the Council on Arteriosclerosis, American Heart Association. Circulation 1995;92:1355–74.
23. McEnery MW, Snowman AM, Trifiletti RR, Snyder SH. Isolation of the mitochondrial benzodiazepine receptor: association with the voltage-dependent anion channel and the adenine nucleotide carrier. Proc Natl Acad Sci U S A 1992;89:3170–4.
24. Zavala F, Lenfant M. Benzodiazepines and PK 11195 exert immunomodulating activities by binding on a specific receptor on macrophages. Ann N Y Acad Sci 1987;496:240–9.
25. Casellas P, Galiegue S, Basile AS. Peripheral benzodiazepine receptors and mitochondrial function. Neurochem Int 2002;40:475–86.
26. Branley HM, du Bois RM, Wells AU, Jones HA. Peripheral-type benzodiazepine receptors in bronchoalveolar lavage cells of patients with interstitial lung disease. Nucl Med Biol 2007;34:553–8.
27. Bazzichi L, Betti L, Giannaccini G, Rossi A, Lucacchini A. Peripheral-type benzodiazepine receptors in human mononuclear cells of patients affected by osteoarthritis, rheumatoid arthritis or psoriasic arthritis. Clin Biochem 2003;36:57–60.
28. De Vos F, Dumont F, Santens P, Slegers G, Dierckx R, De Reuck J. High-performance liquid chromatographic determination of [11C] 1-(2-chlorophenyl)-*N*-methyl-*N*-(1-methylpropyl)-3-isoquinoline carboxamide in mouse plasma and tissue and in human plasma. J Chromatogr B Biomed Sci Appl 1999;736:61–6.
29. Virsu P, Laitinen I, Pöyhönen T, Någren K, Roivainen A. In vivo biodistribution, biokinetics and blood metabolism of [11C] PK11195 in rats—a PET tracer for peripheral benzodiatsepine receptor. Eur J Nucl Med Mol Imaging 2005;32:S266.